ISSN 1070-3284, Russian Journal of Coordination Chemistry, 2017, Vol. 43, No. 7, pp. 446–452. © Pleiades Publishing, Ltd., 2017.
Original Russian Text © L.I. Yudanova, V.A. Logvinenko, L.A. Sheludyakova, I.V. Korol'kov, A.V. Ishchenko, N.A. Rudina, 2017, published in Koordinatsionnaya Khimiya, 2017, Vol. 43, No. 7, pp. 421–427.

Regularities of Thermolysis for the Fe(II), Co(II), and Ni(II) Salts of Maleic and *ortho*-Phthalic Acids with the Formation of Metal/Polymer Composites

L. I. Yudanova[a, *], V. A. Logvinenko[a, b], L. A. Sheludyakova[a, b], I. V. Korol'kov[a, b], A. V. Ishchenko[b, c], and N. A. Rudina[c]

[a] *Nikolaev Institute of Inorganic Chemistry, Siberian Branch, Russian Academy of Sciences, pr. akademika Lavrent'eva 3, Novosibirsk, 630090 Russia*

[b] *Novosibirsk State University, ul. Pirogova 2, Novosibirsk, 630090 Russia*

[c] *Boreskov Institute of Catalysis, Siberian Branch, Russian Academy of Sciences, pr. akademika Lavrent'eva 5, Novosibirsk, 630090 Russia*

**e-mail: judanova@niic.nsc.ru*

Received August 30, 2016

Abstract—Regularities of the thermolysis of acidic salts of unsaturated (maleic) $[M(H_2O)_4(C_4H_3O_4)_2]$ and aromatic (*ortho*-phthalic) $[M(H_2O)_6](C_8H_5O_4)_2$ (M = Fe(II), Co(II), and Ni(II)) acids are established. The thermolysis of both maleates and phthalates can conventionally be divided into three stages. The onset decomposition temperature of the maleates is insignificantly higher than that of the phthalates for the salts of similar metals. The onset dehydration temperature increases in the series of the acidic transition metal maleates and phthalates Fe < Co < Ni, whereas the decarboxylation temperature decreases in the series Fe > Co > Ni. Composites consisting of a metal, an organic polymer, and amorphous carbon are the thermolysis products of both maleates and phthalates in a helium flow. The composites with iron and cobalt in the polymer contain nanosized metal particles and oxide nanoparticles, whose content increases in the composites obtained by the decomposition of phthalates, whereas only metal nanoparticles are observed in the composite with nickel. The compositions and structures of the carbon/polymer matrix differ in these composites.

Keywords: thermolysis, maleates, phthalates, transition metals, nanoparticles, metal/polymer composites

DOI: 10.1134/S1070328417070107

INTRODUCTION

The trend combining the search for precursors (chemical self-controlled systems) and the study of their thermal decomposition is being actively developed in the recent decades [1–4].

A practical significance of this problem is the preparation of composites by the thermolysis of these compounds. The composites contain nanosized particles (≤10 nm) stabilized by the carbon/polymer matrix and additionally enclosed by a graphene or polymer shell. This shell along with the matrix provides nanoparticle encapsulation, which is an important fact, since the high dispersion of metals in the composites results in their strong interaction with components of the medium during both preparation and further storage.

The functional properties of the composites containing metal nanoparticles stabilized by the polymer matrix predetermine their promising use in aerospace technology, microelectronics, and catalysis [5–8].

Salts of carboxylic acids of transition metals Fe(II), Co(II), and Ni(II) can be used as precursors for the preparation of composites by this method. The solution of the problem of the synthesis of the composites containing matrix-stabilized nanoparticles includes the study of the influence of the structure and properties of the precursors on the kinetic regularities and decomposition mechanism and, hence, on the composition, structure, and dispersion of the thermolysis products.

It was shown [1, 2, 9–12] that the thermolysis of Fe(III), Co(II), and Ni(II) acrylates and Co(II) (normal) and Fe(III) (acidic) maleates in the self-generated atmosphere afforded composites, whose metal-containing component was represented by oxide nanoparticles with the diameter that did not exceed 50 nm for the acrylates and 20 nm for the maleates. The polymer matrix of the composites has a cross-linked structure with a system of conjugated multiple bonds. The composition of the polymer matrix for the acrylates is R–[–CH_2–CH–CH_2–CH–]$_{x2}$–R (R =

·CH=CH–CH=CH·), and that for the maleates is –CH=C–(–CHCH–)$_n$–C=CH–.

The thermolysis in a He atmosphere of normal Co(II) and Ni(II) and acidic Fe(II), Co(II), and Ni(II) maleates affords composites containing metal nanoparticles inserted into the polymer matrix. The spherical iron particles are up to 150 nm in size, the size of the cobalt particles is 3–4 nm, and that of the nickel particles is 4–5 nm. An insignificant compaction of the polymer matrix is observed around the iron nanoparticles, whereas the cobalt and nickel nanoparticles have the polymer and graphene shells, respectively. The carbon/polymer matrix with the cross-linked structure includes (–CH=CH–(C)$_x$–·)$_n$ fragments [13]. It was shown for the thermolysis of normal $[Co(H_2O)_2(C_4H_2O_4)](H_2O)$ and acidic $[Co(H_2O)_4(C_4H_3O_4)_2]$ maleates that no polymer shell was formed around the cobalt nanoparticles inserted into the polymer matrix upon the decomposition of the non-single-phase (crystals + substance amorphous to X-rays) samples [14].

The task of the present study is to compare the regularities of the thermal decomposition of the Fe(II), Co(II), and Ni(II) salts of maleic (unsaturated) and *ortho*-phthalic (aromatic) acids aimed at preparing composites containing metal nanoparticles inserted into the carbon/polymer matrix with specified structures and properties.

EXPERIMENTAL

Crystals of acidic Fe(II), Co(II), and Ni(II) maleates and phthalates were obtained by growing from aqueous solutions using a described procedure [4, 14].

It was found by elemental and X-ray phase analyses that the composition of the acidic salts corresponded to the formula $[M(H_2O)_4(C_4H_3O_4)_2]$ for maleates, and that for phthalates was $[M(H_2O)_6](C_8H_5O_4)_2$ (M = Fe(II), Co(II), and Ni(II)).

The content of metals in the precursors and composites was determined by the atomic absorption method on a Z-8000 AA spectrophotometer. Elemental analyses to carbon and hydrogen were carried out on a Euro EA 3000 CHN analyzer. The determination accuracy in two methods was ±0.5 wt %.

The X-ray study of both the starting salts and decomposition products was carried out on a DRON-UM1, a DRON-3M, and a Shimadzu XRD-7000 diffractometers (CuK_α radiation, Ni filter, room temperature).

The thermal decomposition processes were studied by the thermogravimetric (TG), differential thermal analysis (DTA), and differential thermogravimetric (DTG) methods in a He flow on a C derivatograph (MOM, Hungary) with heating to 450°C (accuracy of temperature measurement ±10°C). The weight of the samples in experiments was varied from 20 to 50 mg with an accuracy of weight loss determination of ±0.1% and a heating rate of 2–10 K/min (ceramic microcrucible as a sample holder, helium flow rate 60 cm^3/min). Intermediate phases were characterized by chemical analysis, X-ray diffraction analysis, X-ray phase analysis, and IR spectroscopy. Gaseous products were characterized by mass spectrometry.

The IR spectra of the precursors and composites were recorded on a Vertex 80 FT-IR spectrometer in a range of 400–4000 cm^{-1}. Samples were prepared as pellets with KBr.

The gaseous products of the decomposition of the transition metal maleates and phthalates were studied on a MI-1201 mass spectrometer in a vacuum of 5×10^{-8}–10^{-7} Torr with the temperature increase to ~350°C.

The products of the thermal decomposition of the compounds were studied at different stages by scanning electron microscopy (SEM) on a JSM-6460LV microscope (JEOL, Japan) and high-resolution transmission electron microscopy (TEM) on a JEM-2010 microscope (JEOL, Japan) with an accelerating voltage of 200 keV and a grid resolution of 1.4 Å.

The electron-probe X-ray microanalysis (EDX) of the elemental composition of the samples was carried out on a Phoenix spectrometer with the Si(Li) detector and an energy resolution of about 130 eV.

RESULTS AND DISCUSSION

Acidic maleates $[M(H_2O)_4(C_4H_3O_4)_2]$ (M = Fe(II), Co(II), and Ni(II)) are isostructural and crystallize in the triclinic crystal system (space group $P\bar{1}$, $Z = 1$) [4, 14–17]. The optimization of the growth conditions by the variation of the temperature and pH of the medium made it possible to obtain the isostructural series of acidic phthalates $[M(H_2O)_6](C_8H_5O_4)_2$ with similar cations, whose unit cell parameters were calculated in terms of the monoclinic crystal system (space group $P2_1/c$, $Z = 4$) [18–20].

In the structures of the acidic Fe(II), Co(II), and Ni(II) maleates, the metal atom is located at the center of a slightly distorted octahedron, whose vertices are occupied by four oxygen atoms of the water molecules and two oxygen atoms of the monodentate ligands of maleic acid. The stabilization of the seven-membered ring of each ligand is favored by the short intramolecular hydrogen bond O···H–O. The O···O distance increases insignificantly in the series of the acidic maleates (from 2.426 to 2.436 Å). The linking of the oxygen atoms of the carboxyl and hydroxyl groups by intermolecular hydrogen bonds results in the formation of a porous cross-linked structure [4, 15].

The structures of the acidic phthalates of similar transition metals are layered. The coordination polyhedra of the metal atoms are slightly distorted octahedra with the oxygen atoms of the H_2O molecules in the

vertices. The layer of the octahedra is joined by hydrogen bonds with one of the double layers of the phthalate anions. In another layer, the carboxyl groups are turned toward the octahedral plane and join the biphthalate anions into chains by hydrogen bonds as well [18–20]. No intramolecular hydrogen bond was observed in the anion.

The difference in bond lengths between the metal atom and oxygen atoms of the water molecules should be mentioned for the structures of both acidic maleates and phthalates. For example, the M–O(H_2O) distances in the coordination octahedron of the acidic Co(II) and Ni(II) maleates are 2.043(1), 2.129(1) and 2.024(1), 2.083(1) Å, respectively [17]. At the same time, in the acidic phthalates these distances are somewhat longer for the cobalt (from 2.054(1) to 2.182(1) Å) and nickel (from 2.036(1) to 2.095(1) Å) compound [19, 20]. The M–O(ligand) bond lengths in the structures of the acidic maleates decrease from Fe(II) (2.157(1) Å) to Ni(II) (2.078(1) Å) [17].

A comparison of the thermolysis of the acidic Fe(II), Co(II), and Ni(II) maleates and phthalates (Fig. 1) on heating in a He atmosphere to 450°C made it possible to establish that these processes can conventionally be divided into three stages in both cases. The stepwise dehydration of coordinated water at the first stage of both compounds is determined by structural factors. The decomposition at the second stage is accompanied by the elimination of 50% carboxylate anions (maleate or phthalate anions, respectively). The decarboxylation of the salts at the third stage is accompanied by the formation and growth of metal nuclei and polymerization of organic products.

The higher temperatures of the dehydration onset of the acidic transition metal maleates compared to those for the acidic phthalates at a fairly small difference in the M–O(H_2O) bond lengths in the coordination octahedron can be explained by intermolecular hydrogen bonds in the maleate structures. In the series of transition metals, the temperatures increase for both maleates (Fe (65, 100°C) < Co (70, 110°C) < Ni (105, 130°C)) and phthalates (Fe (50, 65°C) ≤ Co (50, 75°C) < Ni (75, 105°C)), which is consistent with the structural parameters: the M–O_{water} bond lengths decrease in this series.

The chemical, IR spectroscopic, and X-ray phase analyses of the intermediate phase and the comparison of the weight loss in the TG curve with the theoretical value show that no complete H_2O removal (ν(OH) = 3400 cm^{-1}) occurs after the end of the dehydration of all compounds. The diffraction patterns indicate that all samples are amorphous to X-rays at the end of the first stage.

According to the thermogravimetric and mass spectrometric data, for the decomposition of both acidic maleates and phthalates, 50% carboxylate anions are eliminated at the second stage and undergo the further destruction. The gaseous decomposition products of the acidic maleates are vapors of H_2O, maleic anhydride $C_4H_2O_3$, acetylene C_2H_2, CO, CO_2, and aldehydes of propanedionic ($CH_4(CO)_2$) and

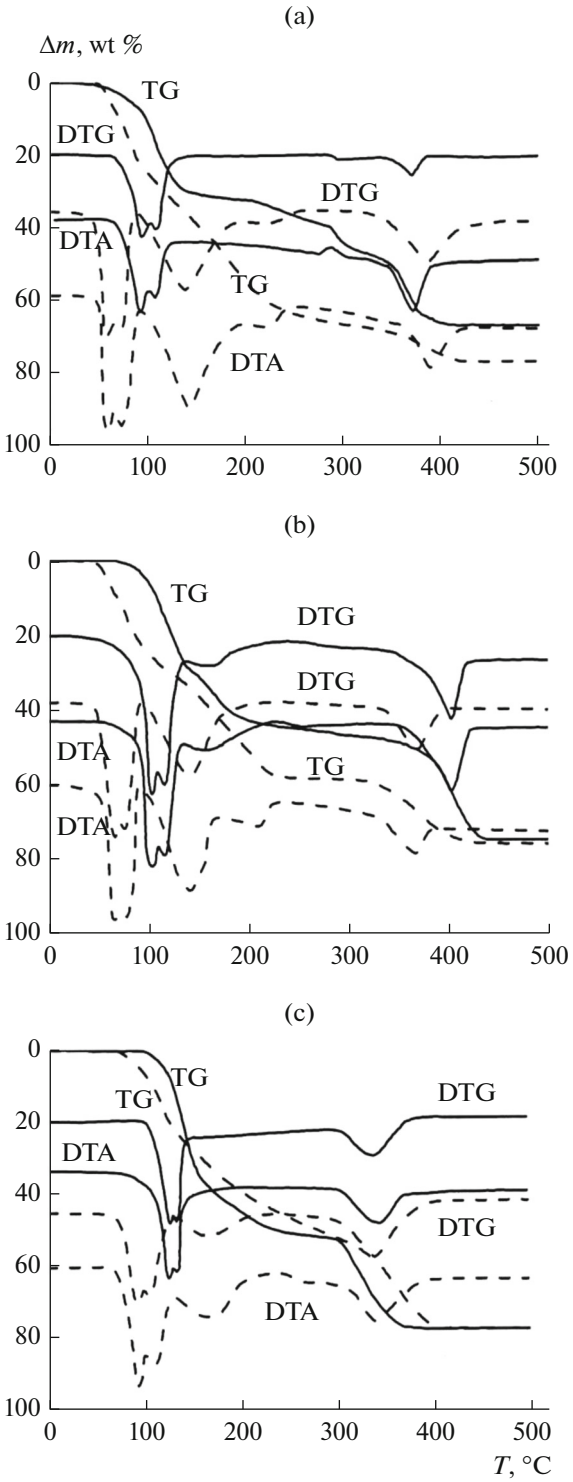

Fig. 1. Thermograms of the decomposition of the acidic (——) maleates and (– – –) phthalates: (a) Fe(II), (b) Co(II), and (c) Ni(II).

acetylenecarboxylic (C_2H_2CO) acids. In the acidic phthalates, the eliminated half of the phthalate dianions decomposes to water and phthalic anhydride.

The higher onset decomposition temperatures at the second stage for the acidic maleates compared to the acidic phthalates can be explained by the coordination bond between the metal atom and oxygen atoms of the carboxyl groups in the structures of the maleates [4]. In the structures of the acidic phthalates, the metal atom in the octahedron is coordinated only by the oxygen atoms of the H_2O molecules. The onset decomposition temperatures in the series of the acidic salts increase at this stage: for maleates, Fe (120°C) < Co (125°C) < Ni (140°C); and for phthalates, Fe (90°C) < Co (100°C) < Ni (135°C).

The absorption spectra of the acidic maleates and phthalates after the second stage are identical to the spectra of the dehydrated normal salts, indicating that the latter are intermediate phases [4, 21].

The decarboxylation of the acidic maleates at the third stage starts almost at the same temperature as that for the phthalates. In the series of the transition metal salts, the temperatures decrease: for maleates, Fe (355°C) > Co (350°C) > Ni (300°C); and for phthalates, Fe (365°C) > Co (340°C) > Ni (300°C).

An analysis of the thermogravimetric, IR spectroscopic, and mass spectrometric data indicates that the last decomposition stage of the acidic maleates and phthalates proceeds in two steps. The diffraction patterns of the decomposition products of the salts contain reflections of the metals already at the initial stage, and the reflection intensity increases as the process occurs.

The studies by the SEM, TEM, and EDX methods showed that, in both cases, the decarboxylation at this stage was accompanied by the growth of metal nuclei and polymerization of organic thermolysis products to form both the carbon/polymer matrix and a polymer or graphene shell around the nanoparticles.

The gaseous products of the decomposition of the acidic Fe(II), Co(II), and Ni(II) maleates at the third stage are similar to the products at the second stage. The thermolysis of the acidic phthalates is accompanied by the evolution of CO_2, diphenylene $C_{12}H_8$, and fluorene $(C_6H_4)_2CH_2$.

In all cases, the composites, being solid residues of decomposition, are black powders consisting of the metal-containing component, organic polymer, and amorphous carbon.

The α-Fe modification with an impurity of oxides Fe_2O_3 and Fe_3O_4 was found by the X-ray phase analysis in the composites upon the decomposition of the acidic Fe(II) maleates and phthalates. The composites obtained by the decomposition of the Co(II) compounds contain the β-Co modification and impurities of the α-Co modification and two oxide phases: CoO and Co_3O_4. The content of O_2 in the composites obtained by the decomposition of the acidic iron and cobalt phthalates is 1.8 and 0.5 wt %, respectively, compared to 0.7 and 0.1 wt % in the composites prepared by the decomposition of the acidic maleates of similar metals. Only metallic nickel is formed by the decomposition of the Ni(II) maleates and phthalates.

The compositions of the metal component in the composites obtained by the decomposition of the maleates and phthalates differ unsubstantially, whereas the differences in the compositions and structures of the polymer matrix are drastic. The C : H ratio in the composites with Fe and Co obtained by the decomposition of the acidic maleates is ~3 : 2, the ratio is 5 : 2 in the composite with Ni, whereas this ratio is ~2 : 1 in the composites with iron, cobalt, and nickel formed upon the decomposition of the acidic phthalates.

A distinctive feature of the IR spectra of the composites obtained by the decomposition of the acidic phthalates is the presence of bands at 1585 and 1485 cm^{-1} (ν(C=C)), which can be attributed to the aromatic ring vibrations. All the spectra contain absorption bands in a range of 3030 cm^{-1} assigned to ν(C–H) and 750 cm^{-1} characteristic of the δ(C–H) vibrations. The bands at 1600–1620 cm^{-1} correspond to vibrations of the ν(C=C) multiple bond of alkenes, and weak absorption bands in a range of 1720–1730 cm^{-1} correspond to ν(C=O), which is explained by the oxidation of the carbon groups on the composite surface. It can be assumed that the decomposition of the acidic maleates results in the formation of a matrix containing $(–CH=CH–C–)_n$ fragments, and the decomposition of the acidic phthalates affords $(–(C_6H_4)–C–C–CH=CH–C–C–)_n$ fragments.

It was established by SEM that all composites obtained by the decomposition of the acidic maleates consisted of aggregates with the sizes from 50 nm to several μm, whereas those prepared by the decomposition of the acidic phthalates consist of larger aggregates, whose size reaches several tens of μm (Fig. 2).

The TEM images show that the matrix of the composites obtained by the decomposition of the acidic phthalates is more disordered compared to that of the composites prepared by the decomposition of the acidic maleates. The size of the iron nanoparticles stabilized by the latter almost does not differ for these classes of compounds. The diameter of the cobalt and nickel nanoparticles (Fig. 3) decreases on going from the composites obtained by the decomposition of the acidic phthalates to maleates. The difference in the catalytic activity of the metals explains the absence of a shell around the Fe nanoparticles and the presence of the polymer shell around the Co nanoparticles and the graphene shell around the Ni particles. Spherical polymer layers containing no metal were mainly found in the composites obtained by the decomposition of the acidic phthalates only. Metal-containing nanoparticles without a shell were observed on the composite

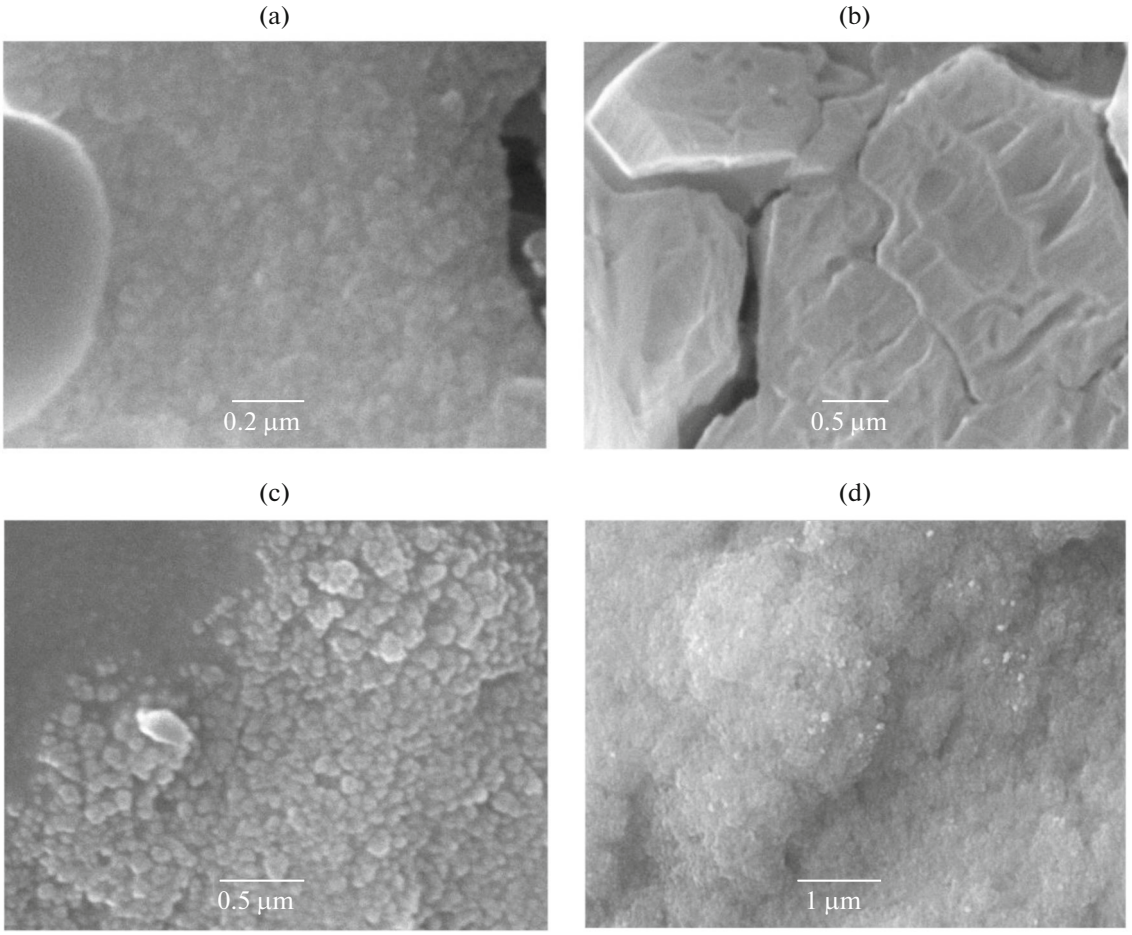

Fig. 2. SEM images of the composites obtained by the decomposition of the acidic maleates and phthalates: (a, c) Co(II) and (b, d) Ni(II).

surface for the decomposition of the acidic Co(II) and Ni(II) phthalates.

The X-ray spectra of the composites obtained by the thermolysis of the acidic phthalates show an increase in the intensity of the OK reflections compared to those of the acidic maleates (Fig. 3).

A comparison of possible routes for thermal transformations during the decomposition of the acidic Fe(II), Co(II), and Ni(II) maleates and phthalates allows one to assume at least two processes in both cases: the radical polymerization of the organic thermolysis products with the formation of the polymer matrix and the catalytic polymerization on the surface of the metal particles.

The processing of the thermogravimetric curves for the third stage of the decomposition of the acidic Co(II) and Ni(II) maleates using the modified Ozawa–Flynn–Wall method indicates in favor of this assumption. The kinetic curves of the reactions in the initial step obey the first-order equation of nucleation $f(\alpha) = (1 - \alpha)$. The second step of the decomposition of acidic cobalt maleate is satisfactorily described by the self-compressed sphere equation $f(\alpha) = (1 - \alpha)^{2/3}$, whereas that of nickel maleate is described by the Prout–Tompkins autocatalytic equation $f(\alpha) = \alpha(1 - \alpha)$ [22, 23], which is consistent with the structure of the composites obtained by the decomposition of these compounds, in particular, by the presence of the polymer shell around the Co nanoparticles and the graphene shell around the Ni nanoparticles.

When processing the curves by the method of the non-isothermal kinetics, the first step of Co(II) phthalate decarboxylation [24] obeys the first-order kinetic equation $f(\alpha) = (1 - \alpha)$, while the second step obeys the Avrami–Erofeev equation $f(\alpha) = (1 - \alpha)[-\ln(1 - \alpha)]^{2/3}$, indicating the reaction mechanism including nucleation followed by the nuclei growth. A specific feature of the decomposition kinetics of dehydrated Ni(II) phthalate [25] is the possibility to describe the decarboxylation step by the second-order equation $f(\alpha) = (1 - \alpha)^2$, which is applicable to reactions in the homogeneous phase and can be extended over the amorphous matrix as well.

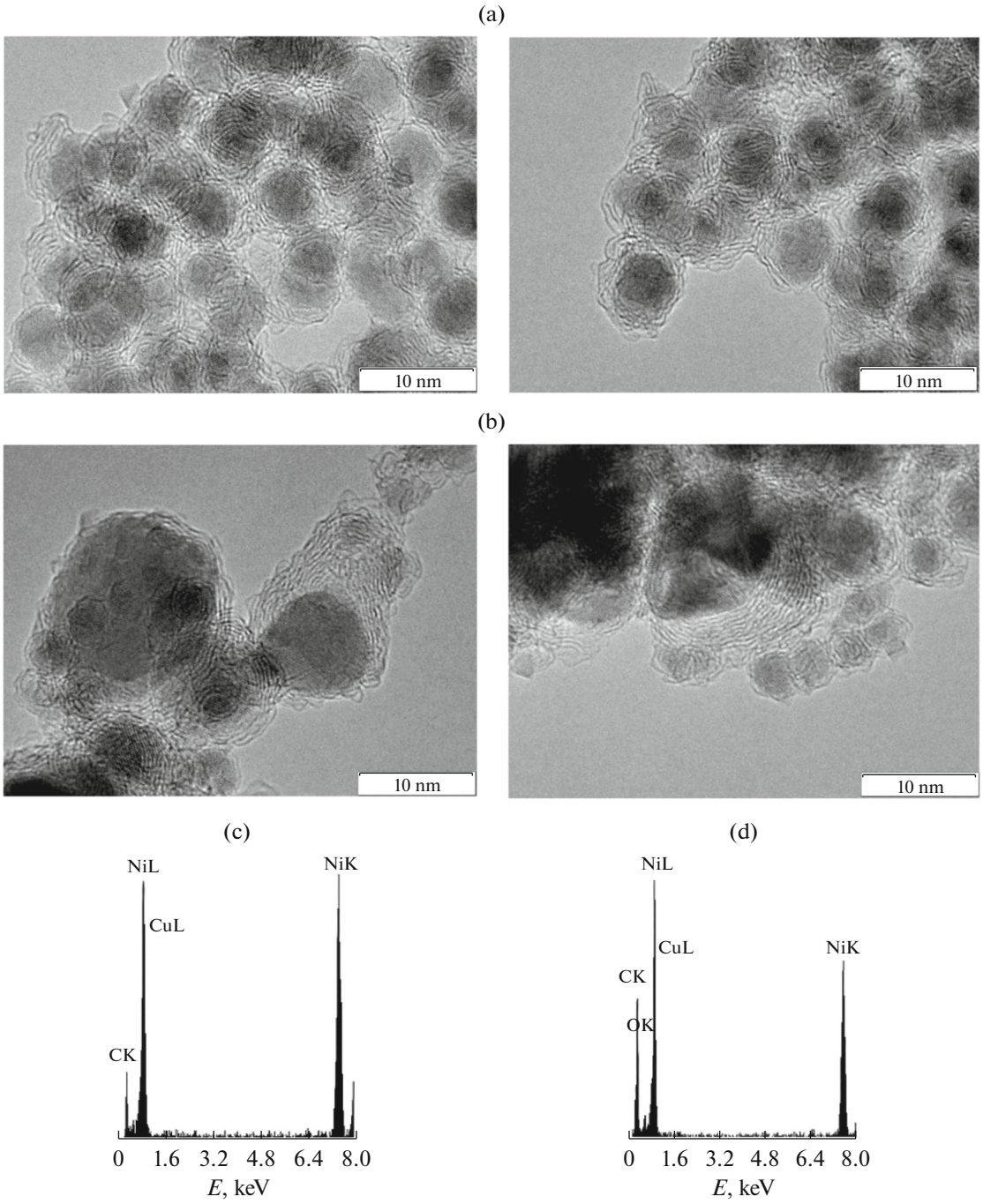

Fig. 3. TEM images and X-ray spectra for the composites obtained by the decomposition of the acidic Ni(II) (a, c) maleate and (b, d) phthalate.

The distinction in the formal kinetic description of the processes can be attributed to the difference in the structures of the composites obtained by the decomposition of the maleates and phthalates. The content of a large amount of cobalt-containing nanoparticles without a shell in the composites obtained by the decomposition of Co(II) phthalate makes it possible to use the geometric model of nuclei growth for the description of the process, whereas the presence of polymer spheres without nickel nanoparticles in the

composites formed upon the decomposition of Ni(II) phthalate is a model for the reactions in the homogeneous phase (Fig. 2).

ACKNOWLEDGMENTS

The authors are grateful to N.F. Beizel', A.P. Zubareva, and O.S. Koshcheeva for conducting elemental analysis.

REFERENCES

1. Pomogailo, A.D. and Kestelman, V.N., *Metallopolymer Nanocomposites*, Berlin-Heidelberg-New York: Springer, 2005.
2. Pomogailo, A.D. and Dzhardimalieva, G.I. *Metallopolimernye gibridnye nanokompozity* (Metallopolymer Hybrid Nanocmposites), Moscow: Nauka, 2015.
3. Porollo, N.P., Aliev, Z.G., Dzhardimalieva, G.I., et al., *Izv. Akad. Nauk., Ser. Khim.*, 1997, no. 2, p. 375.
4. Yudanova, L.I., Logvinenko, V.A., Sheludyakova, L.A., et al., *Russ. J. Inorg. Chem.*, 2014, vol. 59, no. 10, p. 1420.
5. *Nanostrukturnye materialy* (Nanostructured Materials), Khannik, R., Khill, A., Eds., Tekhnosfera, 2009.
6. Fionov, A.S., *Candidate Sci. (Engineering) Dissertation*, Moscow: Institute of Metallurgy and Materials Science, RAS, 2011.
7. Petrov, V., Nikolaichuk, G., Yakovlev, S., and Lutsev, L., *Komp. Tekhnol.*, 2008, no. 10, p. 147.
8. *Nanoparticles and Catalysis*, Astruc, D., Ed., Weinheim: Wiley–VCH, 2008.
9. Pomogailo, A.D., Dzhardimalieva, G.I., Rozenberg, A.S., and Muraviev, D.M., *J. Nanoparticle Res.*, 2003, vol. 5, p. 497.
10. Aleksandrova, E.I., Dzhardimalieva, G.I., Rozenberg, A.S., and Pomogailo, A.D., *Izv. Ross. Akad. Nauk, Ser. Khim.*, 1993, no. 2, p. 308.
11. Rozenberg, A.S., Aleksandrova, E.I., Dzhardimalieva, G.I., et al., *Izv. Ross. Akad. Nauk, Ser. Khim*. 1993, no. 2, p. 1743.
12. Rozenberg, A.S., Aleksandrova E.I., Ivleva N.P., et al., *Izv. Ross. Akad. Nauk, Ser. Khim.*, 1998, no. 2, p. 265.
13. Yudanova, L.I., Logvinenko, V.A., Yudanov, N.F., et al., *Neorg. Mater.*, 2013, vol. 49, no. 10, p. 1138.
14. Yudanova, L.I., Logvinenko, V.A., Yudanov, N.F., USSR Inventor's Certificate No. 2538887, *Byull. Izobret.*, 2015, no. 1.
15. Barman, R.K., Chakrabarty, R., and Das, B.K., *Polyhedron*, 2002, vol. 21, p. 1189.
16. Gupta, M.P., Geise, H.J., and Leustra, A.T.H., *Acta Crystallogr., Sect. C: Cryst. Struct. Commun.*, 1984, vol. 40, p. 1152.
17. Yudanova, L.I., Logvinenko, V.A., Sheludyakova, L.A., et al., *Russ. J. Inorg. Chem.*, 2008, vol. 53, no. 9, p. 1459.
18. Adiwidjaja, G. and Küppers, H., *Acta Crystallogr., Sect. B: Struct. Crystallogr. Cryst. Chem.*, 1976, vol. 32, p. 1571.
19. Adiwidjaja, G., Rossmanith, E., and Kuppers, H., *Acta Crystallogr., Sect. B: Struct. Crystallogr. Cryst. Chem.*, 1978, vol. 34, p. 3079.
20. Yudanova, L.I., Logvinenko, V.A., Semyannikov, P.P., et al., *Russ. J. Coord. Chem.*, 2010, vol. 36, no. 1, p. 22.
21. Yudanova, L.I., Logvinenko, V.A., Yudanov, N.F., et al., *Russ. J. Phys. Chem.*, 2016, vol. 90, no. 6, p. 1206.
22. Janković, B. and Adnadević, B., *Int. J. Chem. Kin.*, 2007, vol. 39, no. 8, p. 462.
23. Logvinenko, V.A., Yudanova, L.I., Yudanov, N.F., and Chekhova, G.N., *J. Therm. Anal. Calorim.*, 2003, vol. 74, p. 395.
24. Acheson, R.J. and Galwey, A.K., *J. Inorg. Nucl. Chem.*, 1968, vol. 30, p. 2381.
25. Galwey, A.K., *J. Catalysis*, 1965, vol. 4, no. p. 697.

Translated by E. Yablonskaya